BoxCar and library-free data-independent acquisition substantially improve the depth, range, and completeness of label-free quantitative proteomics in Arabidopsis

Devang Mehta[1], Sabine Scandola[1] and R. Glen Uhrig[1 #]

Abstract

The last decade has seen significant advances in the application of quantitative mass spectrometry-based proteomics technologies to tackle important questions in plant biology. The current standard for quantitative proteomics in plants is the use of data-dependent acquisition (DDA) analysis with and without the use of chemical labels. However, major limitations of the DDA approach are the preferential measurement higher abundant proteins, and the presence of missing values for proteins measured across replicate and independent samples. Here, we systematically compare and benchmark a state-of-the-art DDA label-free quantitative proteomics workflow for plants against a recently developed direct data-independent acquisition (directDIA) method. Our study demonstrates several advantages of directDIA including a 33% increase in the number of quantified proteins and the elimination of bias against the reproducible quantification of low-abundant proteins—a particularly important finding given the large dynamic range of plant proteomes. We next compared directDIA with a novel approach combining MS^1-level BoxCar acquisition with MS^2-level library-free DIA analysis (BoxCarDIA). Our BoxCarDIA method resulted in an additional 8% increase in the number of proteins quantified over directDIA, with further gains in quantitative completeness. Cumulatively, the methods benchmarked here achieve a 41% increase in protein quantification without any changes in instrumentation, offline fractionation, or increases in mass-spectrometer run time. We also applied directDIA to perform a quantitative proteomic comparison of dark and light grown Arabidopsis cell cultures, providing a critical resource for future plant interactome studies using this well-established biochemistry platform. Our results establish BoxCarDIA and directDIA as the new methods of choice in quantitative proteomics using Orbitrap-type mass-spectrometers.

[1] Department of Biological Sciences, University of Alberta, Edmonton T6G 2E9, Alberta, Canada

[#] Correspondence
Dr. R. Glen Uhrig
ruhrig@ualberta.ca

Keywords
Arabidopsis thaliana, cell culture, proteome, quantitative proteomics, data dependent acquisition, data independent acquisition, BoxCar, mass spectrometry

Funding
This work was funded by the National Science and Engineering Research Council of Canada (NSERC) and the Canadian Foundation for Innovation (CFI).

Introduction

The last decade has seen significant advances in the application of quantitative mass spectrometry-based proteomics technologies to tackle important questions in plant biology. This has included the use of both

label-based and label-free quantitative liquid-chromatography mass spectrometry (LC-MS) strategies in model[1,2] and non-model plants[3]. While chemical labelling-based workflows (e.g. iTRAQ and TMT) are generally considered to possess high quantitative accuracy, they nonetheless suffer from ratio distortion and sample interference issues[4,5], while being less cost-effective and offering less throughput than label-free approaches. Consequently, label free quantification (LFQ) has been widely used in comparative quantitative experiments profiling the native[6] and post-translationally modified (PTM-ome)[7,8] proteomes of plants. However, LFQ shotgun proteomics studies in plants have so far, almost universally, used data-dependent acquisition (DDA) for tandem MS (MS/MS) analysis.

In a typical DDA workflow, elution groups of digested peptide ions (precursor ions) are first analysed at the MS^1 level using a high-resolution mass analyser (such as modern Orbitrap devices). Subsequently, selected precursor ions are isolated and fragmented, generating MS^2 spectra that deduce the sequence of the precursor peptide. For each MS1 scan usually around 10-12 MS^2 scans are performed after which the instrument cycles to the next MS^1 scan and the cycle repeats. While this "TopN" approach enables identification of precursors spanning the entire mass range, the fragmentation of semi-stochastically selected precursor ions (generally, more intense ions) limits the reproducibility of individual DDA runs, results in missing values between replicate runs, and biases quantitation toward more abundant peptides[9]. This is particularly disadvantageous for label-free workflows and samples with a high protein dynamic range, such as human plasma and photosynthetic tissue.

In order to address these limitations, several data-independent acquisition (DIA) workflows have been pioneered, famously exemplified by Sequential Window Acquisition of All Theoretical Mass Spectra (SWATH-MS)[10,11]. In DIA workflows, specific, often overlapping, m/z windows spanning a defined mass range are used to sub-select groups of precursors for fragmentation and MS^2 analysis. As a result, complete fragmentation of all precursors in that window follows MS^1 scans resulting in a more reproducible and complete analysis. A major disadvantage of DIA workflows, however, is that each MS^2 scan contains multiplexed spectra from several precursor ions making accurate identification of peptides difficult. Traditionally, this has been addressed through the use of global or project-specific spectral-libraries obtained from a fractionated, high-resolution DDA survey of all samples—adding to experimental labour and instrumentation analysis time. More recently, alternative approaches have been developed that avoid the use of spectral libraries and instead use "pseudo-spectra" derived from DIA runs that are then searched in a spectrum-centric approach analogous to conventional DDA searches[12–14]. Improvements in such library-free DIA approaches have included the incorporation of high precision indexed Retention Time (iRT) prediction[15] and the use of deep-learning

approaches[16–18]. DirectDIA (an implementation of a library-free DIA method; Biognosys AG) and a hybrid (directDIA in combination with library-based DIA) approach has been recently used to quantify more than 10,000 proteins in human tissue[19] and reproducibly identify >10,000 phosphosites across hundreds of human retinal pigment epithelial-1 cell line samples[20].

While DIA addresses the stochasticity of precursor selection for fragmentation, it does not solve the problem of incomplete MS^1 analysis due to the limited charge capacity of C-traps that lie upstream of Orbitraps. In effect this means that modern Orbitrap mass-spectrometers only analyse <1% of available ions at the MS^1 level[21]. In 2018, Meier et al., described a novel acquisition scheme called BoxCar where multiple overlapping sets of narrow m/z segments are scanned at the MS^1 level followed by conventional DDA-type MS^2 analysis[21]. It is thus reasonable to speculate that combining the power of BoxCar to produce higher-resolution MS^1 data with DIA-type MS^2 analysis (BoxCarDIA) may provide greater quantitative depth and range for shotgun proteomics.

DirectDIA combines the advantages of DIA for reproducible quantification of proteins in complex mixtures with high dynamic range, with the ease of use of earlier DDA methodologies. BoxCarDIA may improve MS^1 resolution and dynamic range, while addressing the limitations of DDA-type precursor fragmentation. Hence, a systematic comparison of these different technologies for LFQ proteomics is essential to define best practice in plant proteomics. In order to execute this analysis, we compared the proteomes of light- and dark-grown Arabidopsis suspension cells generated with DDA, directDIA and BoxCarDIA acquisition schemes. Arabidopsis suspension cells are a long-established platform for plant biochemistry and have recently seen a resurgence in popularity due to their utility in facilitating protein interactomic experimentation using technologies such as tandem affinity purification-mass spectrometry[22–26], nucleic acid crosslinking[27], and proximity labelling (e.g. TurboID)[28]. Despite this, no existing resource profiling the basal differences in proteomes of Arabidopsis cells grown in light or dark exists—a fundamental requirement to determine the choice of growth conditions to maximize the utility of protein interactomic experiments and targeted proteomic assays in this system.

Results & Discussion

We performed total protein extraction under denaturing conditions from Arabidopsis (cv. Ler) suspension cells grown for five days in either constant light or dark. Trypsin digestion of the extracted proteome was performed

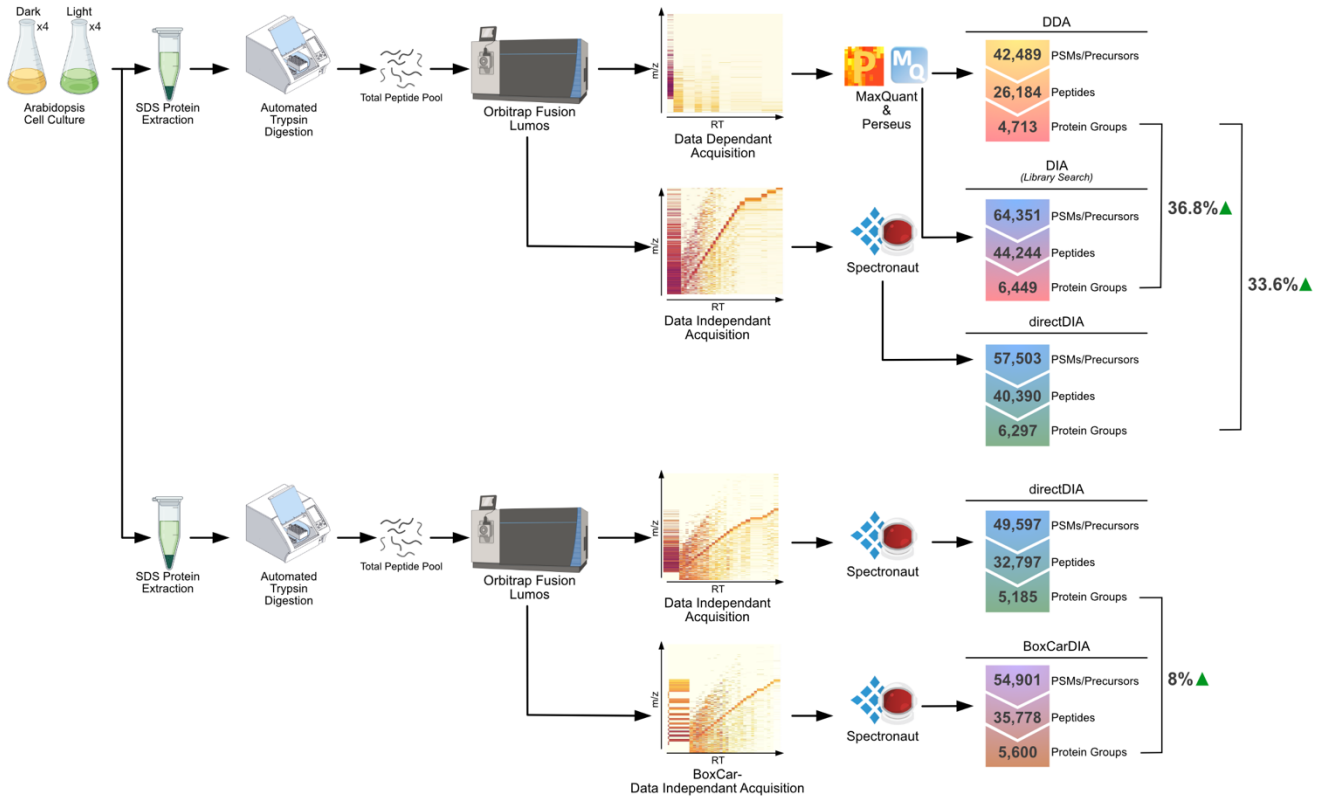

Figure 1: Experimental workflow and summary results.
Total protein was isolated from light and dark grown Arabidopsis cells under denaturing conditions for use in two experiments. In the first experiment, peptides were digested with trypsin, desalted and subjected to LC-MS/MS using two different acquisition modes. Ion maps showing a single MS1 scan and subsequent MS2 scans are presented to illustrate differences in acquisition schemes. Raw data was analyzed using MaxQuant & Perseus for data-dependent acquisition (DDA) analysis and using Spectronaut for data-independent acquisition (DIA) analysis using spectral libraries created from both acquisitions, and for directDIA analysis without the use of spectral libraries. A second experiment involved analyzing independent digests of the same protein extracts followed by the same general analysis pipeline, in order to directly compare directDIA and library-free BoxCarDIA acquisition modes. Counts of FDR-filtered (0.01) peptide spectrum matches (PSMs)/precursors, peptides, and protein groups for each analysis type are shown. Percentage values for increases in protein group quantifications are shown alongside each analysis.

using an automated sample preparation protocol, with 1ug of digested peptide subsequently analysed using an Orbitrap Fusion Lumos mass spectrometer operated in either DDA, DIA, or BoxCarDIA acquisition modes over 120-minute gradients. Two separate experiments were performed using independent digests of the extracted Arabidopsis proteins. The first to compare DDA and directDIA, and the second to compare directDIA with BoxCarDIA. Eight injections (4 light & 4 dark) per analysis (a total of 32 injections) were carried out. DDA data processing was performed using MaxQuant, while DIA data processing was performed using Spectronaut v14 (Biognosys AG.). For DIA analysis, both hybrid (library+directDIA) and directDIA analysis was performed. The hybrid analysis was performed by first creating a spectral library from DDA raw files using the Pulsar search engine implemented in Spectronaut, followed by a peptide-centric DIA analysis with DIA raw output files. DirectDIA was performed directly on raw

DIA files as implemented in Spectronaut. The entire workflow is depicted in **Figure 1**. Both hybrid DIA and directDIA analysis substantially outperformed DDA analysis with an average of 65,351; 57,503; and 42,489 peptide-spectrum matches (precursors) quantified across all 8 samples for each analysis, respectively. Hybrid DIA and directDIA also displayed similar gains over DDA in terms of quantified peptides and protein groups (**Figure 1**). While hybrid DIA analysis performed marginally better than directDIA, further analysis was performed with the results of only direct DIA and DDA analyses in order to compare methods that use an equivalent number of MS raw input files, comparable instrumentation time and relatively comparable data analysis workflows. We also found substantial improvements in quantifying precursors, peptides, and protein groups using BoxCarDIA as compared to directDIA. Overall, our results suggest that library-free BoxCarDIA can increase quantitative depth by as much as 40% over conventional DDA methods with no increase in analysis time or change in instrumentation.

Next, we undertook a series of data analyses to compare the completeness, quality, and distribution of protein group-level quantification of the DDA and directDIA analyses. In order to compare quantification results across the different analysis types, raw intensity values for each sample were $\log_2$ transformed, median-normalized (per sample), and then averaged for each condition to produce a normalized protein abundance value. For DDA analysis, the number of proteins quantified was determined by first filtering for proteins with valid quantification values in at least 3 of 4 replicates in either condition (light or dark) and then imputing missing values using MaxQuant with standard parameters[29,30]. For directDIA and BoxCarDIA analyses, quantified proteins were defined as those passing standard Q-value filtering in Spectronaut. In total, DDA analysis resulted in the quantification of 4,837 proteins (both conditions) and directDIA analysis quantified 6,526 proteins (light) and 6,454 proteins (dark) (**Supplementary Tables 1-3**). Upon comparing the quantified proteins between both methods, we found that 4,599 proteins were quantified by both techniques, 1,934 were quantified only by directDIA and 235 proteins were exclusively DDA-quantified, for light-grown cells (**Figure 2a**). A correlation plot of normalized quantification values for the 4,599 common proteins showed a moderate correlation between DDA and directDIA quantification (Spearman's R = 0.773) (**Figure 2a**). Examining the frequency distribution of proteins quantified in light-grown cells, by both methods, revealed that the DDA results were substantially skewed towards higher abundant proteins compared to directDIA (**Figure 2b**). In order to investigate the overlap of quantified proteins between directDIA and DDA at extreme protein abundances, we sub-selected the 2%, 5%, 95% and 98% percentile of the combined quantification distribution and constructed UpSet plots[31] for these datasets. This analysis revealed that directDIA quantifies hundreds of more proteins at the lower extremes but is only marginally less effective than DDA

at the upper extremes of the protein abundance distribution (**Figure 2c**). These results were similarly replicated for dark-grown cells, suggesting that this is a universal feature of the two acquisition methods, irrespective of sample treatment or type (**Figure 2 d-f**). In order to assess if this difference in quantification ability is specific to plant cells (that have a high dynamic range of protein levels), we further analysed a commercial HeLa cell digest standard using the same mass spectrometry and chromatography settings, with quadruplicate injections per analysis type. Analysing the HeLa quantification results (**Supplementary Tables 4 & 5**) showed a similarly uniform quantification across a wide range by directDIA and a slightly better, but still skewed, performance by DDA compared to Arabidopsis cells (**Figure S1 a & b**). Comparing the quantification values for HeLa proteins acquired by directDIA and DDA showed a stronger correlation than for Arabidopsis (Spearman's R=0.886). Indeed, correlations between quantification values for lower abundant proteins (defined here as proteins below the median quant value), were much lower than for the overall dataset in both species, and yet slightly stronger in the case of HeLa proteins (**Figure S1 c-e**).

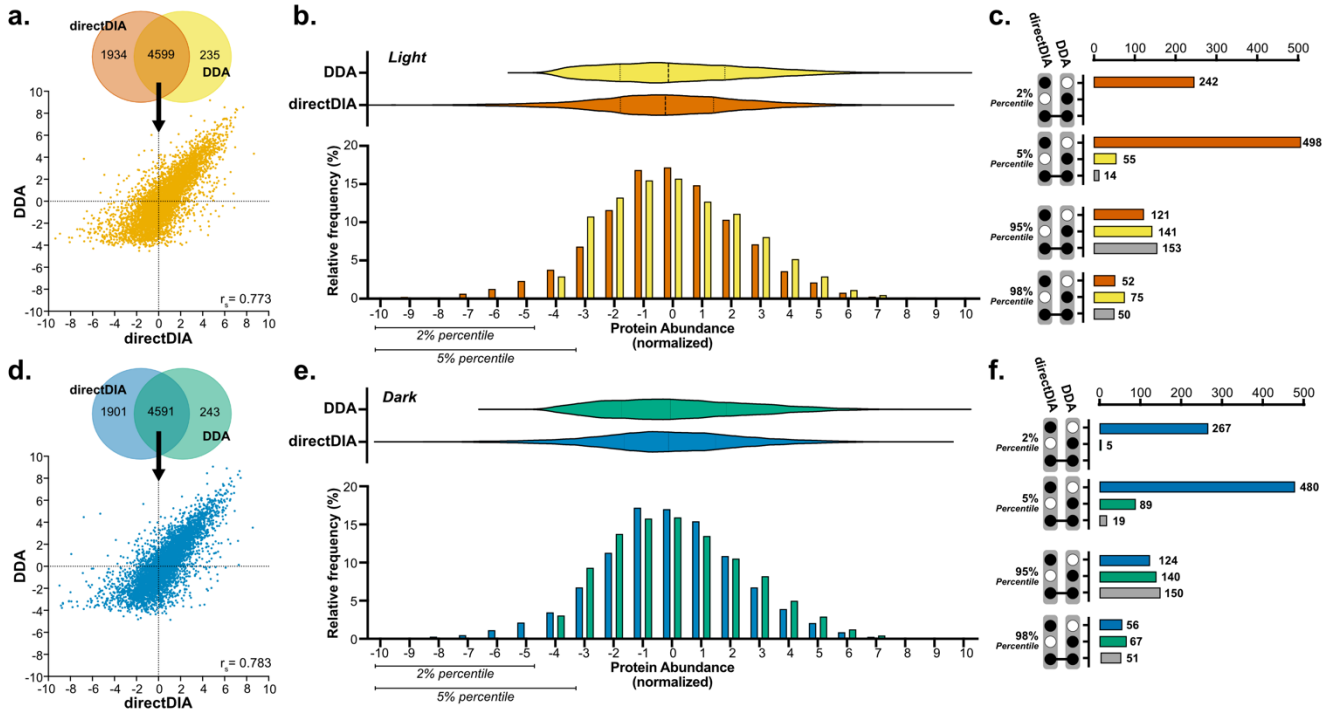

Figure 2: Comparison of protein quantification results using DDA and direct DIA analysis for (a.-c.) light grown and (d.-f.) dark grown Arabidopsis cells.

(a.) & **(d.)** Venn diagram of protein groups quantified with direct DIA and DDA and scatter plot of protein groups quantified by both methods. r_s: Spearman's correlation coefficient. **(b.)** & **(e.)** Frequency distribution of normalized protein abundances for DDA and direct DIA analysis and corresponding violin plots with median and quartile lines marked. **(c.)** & **(f.)** Upset plots depicting intersections in protein groups quantified by DDA and direct DIA at either extremes of the abundance distribution.

We next performed similar comparative analyses for an independent experiment comparing directDIA and BoxCarDIA approaches (**Figure 3**). In this experiment, BoxCarDIA resulted in the quantification of 5,806 (light) and 5,791 (dark) proteins compared to 5,377 (light) and 5,354 (dark) using directDIA (**Supplementary Tables 6 & 7).** The relative abundance of proteins quantified in both analyses correlated to a large degree (Spearman's r ~ 0.92; **Figure 3 a & d**), much more than the correlation between directDIA and DDA analyses (**Figure 2 a & d**). The frequency distributions of normalised abundances of proteins quantified by both directDIA and BoxCarDIA showed that BoxCarDIA is better able to quantify both high- and low-abundant proteins, for both light and dark grown cells (**Figure 3 b & e**). This is clearly evident upon UpSet plot visualization of the overlap between the two techniques at the extremes of the protein abundance distributions (**Figure 3 c & f**).

In order to deduce the underlying factors limiting the ability of DDA to quantify low abundant proteins, especially in Arabidopsis cells, we next investigated quantification distributions for both DDA and directDIA derived data after various data-filtering steps (**Figure S2**; **Supplementary Tables 8-17**). We found that DDA was indeed able to identify a similar number of proteins as directDIA for both Arabidopsis cells and HeLa digests.

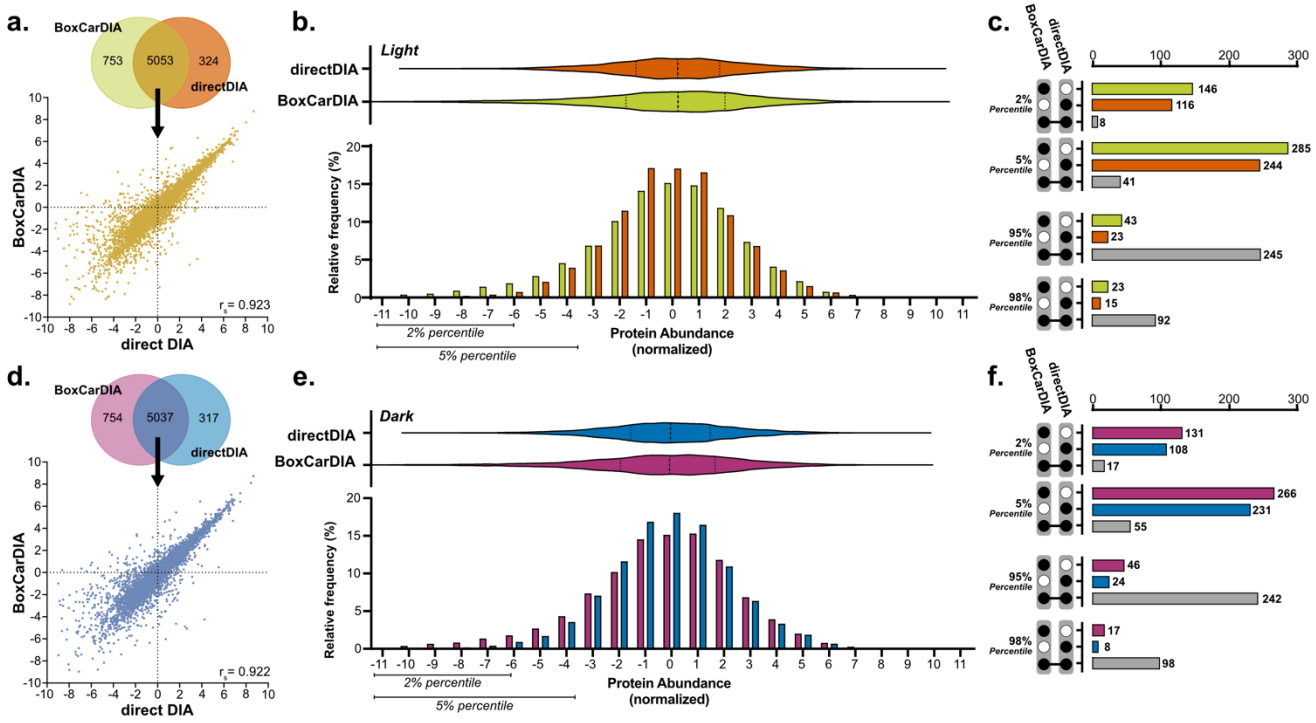

Figure 3: Comparison of protein quantification results using directDIA and BoxCarDIA analysis for (a.-c.) light grown and (d.-f.) dark grown Arabidopsis cells.
(a.) & **(d.)** Venn diagram of protein groups quantified with BoxCarDIA and directDIA, and scatter plot of protein groups quantified by both methods. r_s: Spearman's correlation coefficient. **(b.)** & **(e.)** Frequency distribution of normalized protein abundances for directDIA and BoxCarDIA analysis and corresponding violin plots with median and quartile lines marked. **(c.)** & **(f.)** Upset plots depicting intersections in protein groups quantified by directDIA and BoxCarDIA at either extreme of the abundance distribution.

Predictably these numbers dropped dramatically upon filtering proteins for only those with valid quantification values across 3 of 4 replicates, with only mild gains realized due to imputation of missing values. In contrast, even upon filtering for valid values across 4 of 4 replicates, directDIA resulted in the quantification of more than 5,400 proteins compared to 3,600 complete quantifications for DDA. Strikingly, quantification distributions remained unchanged regardless of various types of data-filtering for directDIA but were greatly skewed towards high abundance upon filtering for valid values in 3 of 4 replicates in DDA outputs (**Figure S2**). This suggests that the poor quantification of low abundant proteins is related to the presence of missing values in DDA analysis.

This hypothesis was reinforced when we distributed the protein quantification data for directDIA and DDA based on the number of replicates with valid quantification values for each protein (**Figure 4**). Here we found that the overwhelming majority (>95%) of proteins quantified by directDIA had valid values in at least 3 of 4 biological replicates for Arabidopsis cells grown in the light or dark (**Figure 4 a & b**). Unsurprisingly, in the HeLa digest, more than 98% of directDIA quantified proteins were accurately quantified in 4 of 4 technical injections. In contrast, only 68% and 74% of proteins were accurately quantified by DDA in 4 of 4 replicates of light and dark grown Arabidopsis cells, respectively. In fact, the distribution of protein quantification was bimodal, with as many as 17% of proteins accurately quantified in only 1 of 4 replicates by DDA in light-grown cells (10.9% in dark-grown cells). Nearly a quarter of proteins were accurately quantified by DDA in only 1 of 4 technical injections of the same HeLa cell digest, suggesting an inherent disadvantage in reproducibility across replicate runs. In contrast, no proteins were quantified in only 1 of 4 technical injections of the same HeLa digest when using directDIA and 99.4% were quantified in 4 of 4 technical replicates. When these distributions were further plotted against the normalized protein quantification values, it became clear that proteins found in a lower number of replicates trended lower in abundance in DDA, while this trend did not hold true for directDIA (**Figure 4 d-i**). In the case of directDIA, a greater number of quantified proteins were found in 1 of 4 or 2 of 4 biological replicates in Arabidopsis cells compared the technical replicates of HeLa digests. This suggests that the inconsistent quantification of some low abundant proteins using directDIA is a reflection of real biological variance rather than a methodological artefact. This is contrary to DDA where similar proportions of low abundant proteins were inconsistently identified across biological replicates of Arabidopsis cells and technical replicates of HeLa digests. Overall, this further reinforces that DDA acquisition results in inconsistent quantification between injections, and that this may in fact obscure real biological variance between samples, especially with regards to lower abundant proteins.

In order to assess whether BoxCarDIA could achieve further gains in quantitative completeness, we performed 4 technical replicate injections of HeLa digests using each, BoxCarDIA and directDIA acquisition. Similar to our previous analysis, the vast majority of proteins quantified by directDIA were found in all 4 replicates (**Figure 5a; Supplementary Tables 18 & 19**). The relationship between quantitative completeness and relative abundance is also maintained as in the case of our prior analysis (**Figure 5b**). However, BoxCarDIA showed remarkable improvements in data completeness even compared to directDIA with all but one protein quantified in all four replicates (**Figure 5 a & c**). This result shows that the gains in quantitative depth and range provided by better sampling of the ion beam at the MS^1 level

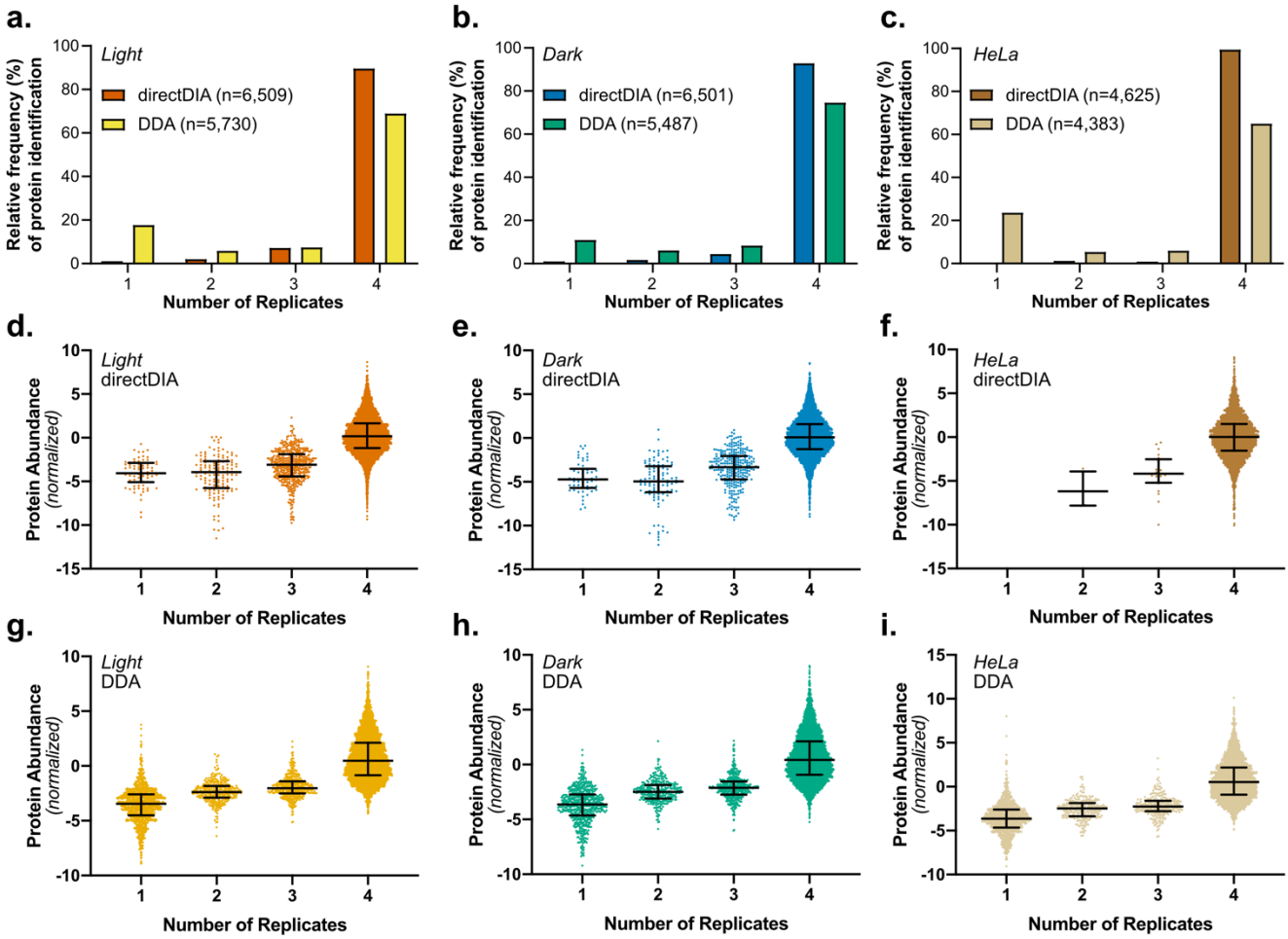

Figure 4: The DDA missing value problem explains the gap in quantification of low abundant proteins compared to direct DIA. (a.-c.) Histograms of direct DIA or DDA protein group identifications across replicate samples for light-grown, dark-grown Arabidopsis cells, and HeLa cell digestion standards, respectively. **(d.-i.)** Normalized abundances of proteins binned by the number of replicates containing each protein for direct DIA and DDA. Bars represent median and interquartile range.

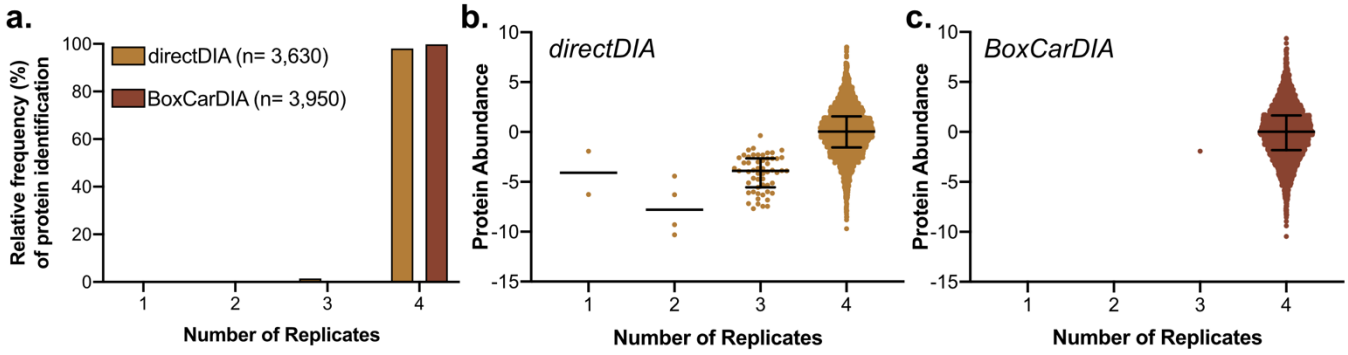

Figure 5: BoxCarDIA can quantify proteins consistently between independent technical replicate injections. (a.) Histograms of BoxCarDIA or directDIA protein group identifications across replicate injections of HeLa cell digestion standards. **(b & c.)** Normalized abundances of proteins binned by the number of replicates containing each protein for directDIA and BoxCarDIA. Bars represent median and interquartile range.

in BoxCarDIA also translate to a complete data matrix, entirely eliminating the long-standing missing-value problem in label-free quantitation.

Having systematically investigated the advantages and limitations of BoxCarDIA, directDIA and DDA acquisition for LFQ proteomics, we next performed a differential abundance analysis comparing the proteomes of light- and dark-grown cell cultures quantified in our initial directDIA and DDA experiment. We found 2,089 proteins changing significantly in their abundance (Absolute Log2FC > 0.58; q-value <0.05) in our directDIA analysis and 1,116 proteins changing significantly (Absolute Log2FC > 0.58; q-value <0.05) in DDA analysis. Of these, 710 proteins were found to change significantly in both analyses (**Figure 6a**). The Log_2 Fold-Change values of these 710 proteins were found to correlate to a high degree between the two analyses (Spearman's R=0.9003), with proteins that were up-regulated in light- vs. dark-grown cells in directDIA analysis also up-regulated in DDA, and vice-versa (**Figure 6b**). This complete dataset of 2,495 proteins changing significantly in abundance in light- vs dark-grown Arabidopsis cells is a valuable resource for future biochemical studies aiming to use these cell culture systems for protein interactomics experiments and other targeted proteomics analyses (**Supplementary Table 20**). We also created a functional association network of these proteins by probing previously characterized databases and experiments compiled by StringDB[32]. This network validates our analysis, showing that clusters of proteins involved in photosynthesis, carbon-fixation, starch metabolism and amino-acid metabolism have increased abundance in light- vs. dark-grown cells, as expected (**Figure 6c**). Interestingly, clusters representing RNA splicing, ER-Golgi transport, ribosome biogenesis, and nuclear translation are all downregulated, while chloroplast translation is upregulated, in light- vs. dark-grown cells (**Figure 6c**).

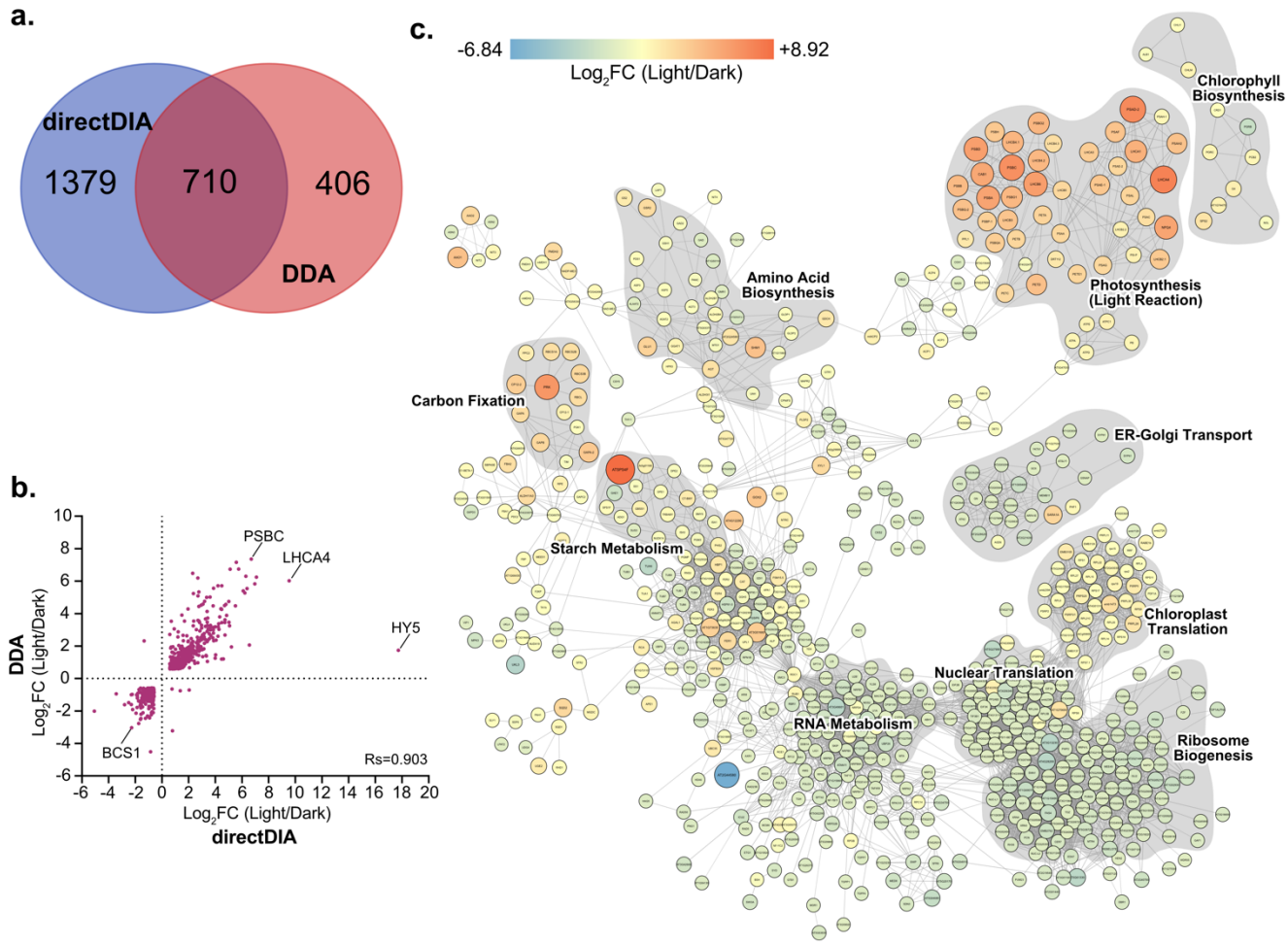

Figure 6: Differential protein abundance analysis for light- and dark-grown Arabidopsis cells.
(a.) Venn diagram of protein groups with significantly changing protein abundances (q<0.01; Abs Log_2FC>1.5) as measured by direct DIA and DDA. **(b.)** Scatter plot of significant changes in protein abundance changes based on DDA and direct DIA analysis with selected proteins labeled. **(c.)** Association network of significantly changing proteins detected with either direct DIA or DDA analysis. Network was constructed based on StringDB database and experiment datasets with a probability cut-off of 0.8. Only nodes with >3 edges are depicted. Clusters were manually annotated based on GO-terms and KEGG/Reactome pathway membership. Node sizes and color are scaled based on the average Log_2FC (Light/Dark) from DDA and DIA analysis.
PSBC: PHOTOSYSTEM II REACTION CENTER PROTEIN C; LHCA4: LIGHT-HARVESTING CHLOROPHYLL-PROTEIN COMPLEX I SUBUNIT A4; HY5: ELONGATED HYPOCOTYL 5; BCS1: CYTOCHROME BC1 SYNTHESIS

Discussion

Until recently, DDA proteomics (using both label-based and label-free approaches) was clearly the method of choice for functional genomics studies in plants, due to the disadvantages of conventional DIA analysis, such as the requirement for project-specific spectral libraries. Here, we conclusively demonstrate that the newly developed directDIA proteomics approach is a vastly superior technique for plant proteomics as compared to currently used DDA methodologies. We also demonstrate that our novel library-free BoxCarDIA method substantially improves upon gains provided by directDIA. The advantages offered by directDIA and BoxCarDIA include a

greater number of protein identifications, more dynamic range, and more robust protein quantification than DDA, with no change in instrumentation or increase in instrument analysis time. Our DDA results, even using an advanced Tribrid Orbitrap-linear ion trap device, show that DDA acquisition is particularly inconsistent in its quantification of low-abundant proteins across samples. Similar results have been reported when comparing the abilities of directDIA and DDA to profile the phosphoproteome (a protein fraction with high dynamic range) of human tissue and cells [20]. Our finding that more than 20% of identified proteins in a DDA experiment are found in only 1 of 4 replicate injections of the same digest, and that these poorly quantified proteins tend to reside in the lower quartile of protein abundance, suggests an inherent drawback in DDA that likely plagues previous studies using this approach, in both label-free and label-based incarnations. Further, the greater proportion of missing values in light- vs. dark-grown cells with both DDA and DIA analysis suggests that the effect of ion suppression is greater in photosynthetically active tissue (**Figure 4 a & b**).

The directDIA and BoxCarDIA acquisition methods are compatible with a wide range of modern mass spectrometers, including older Orbitrap (e.g., QExactive Orbitrap mass spectrometers; ThermoScientific) and Triple TOF devices (Sciex). The various data analyses undertaken in our plant proteomic study provide a useful template for benchmarking these future quantitative mass-spectrometry proteomics technologies from an end-user perspective. While our results demonstrate that segmented MS^1 analysis through the use of BoxCar windows results in a variety of gains, there are likely further improvements in BoxCarDIA that may be realised through the use of better signal processing methods in order to reduce cycle times[33,34].

In the meantime, our results argue persuasively for the widespread adoption of library-free BoxCarDIA or directDIA for quantitative LFQ proteomics in plants. It should be noted that while we utilized proprietary software for directDIA analysis (Spectronaut v.14, Biognosys AG), multiple free open-source alternatives exist[12,13,17,18] and proprietary software are often available to scientists via professional mass-spectrometry facilities. The demonstrated benefits in reproducibility and dynamic range of BoxCarDIA could be especially powerful for plant biology studies such as the proteomic analysis of multiple treatments (e.g., plant nutrition or herbicide studies), genotypes (e.g. breeding and selection trials), or timepoints (e.g. chronobiology studies).

Methods

Arabidopsis cell culture

Heterotrophic *Arabidopsis thaliana*, cv. Ler suspension cells were obtained from the Arabidopsis Biological Resource Center (ABRC) and maintained in

349 standard Murashige-Skoog media basal salt mixture (M524; PhytoTech
350 Laboratories) at 21 °C as previously described[35] under constant light (100
351 µmol $m^{-2}s^{-1}$) or constant dark. For the generation of experimental samples,
352 10 mL aliquots of each cell suspension (7 days old) were used to inoculate 8
353 separate 500 mL flasks that each contained 100 mL of fresh media.
354 Experimental samples were grown for an additional 5 days prior to
355 harvesting. Cells were harvested by vacuum filtration and stored at −80 ºC.

356 ## Sample Preparation

357 Quick-frozen cells were ground to a fine powder under liquid N_2 using a
358 mortar and pestle. Ground samples were aliquoted into 400 mg fractions.
359 Aliquoted samples were then extracted at a 1:2 (w/v) ratio with a solution of
360 50 mM HEPES-KOH pH 8.0, 50 mM NaCl, and 4% (w/v) SDS. Samples were
361 then vortexed and placed in a 95ºC table-top shaking incubator (Eppendorf)
362 at 1100 RPM for 15 mins, followed by an additional 15 mins shaking at room
363 temperature. All samples were then spun at 20,000 x g for 5 min to clarify
364 extractions, with the supernatant retained in fresh 1.5 mL Eppendorf tubes.
365 Sample protein concentrations were measured by bicinchoninic acid (BCA)
366 assay (23225; ThermoScientific). Samples were then reduced with 10 mM
367 dithiothreitol (DTT) at 95ºC for 5 mins, cooled, then alkylated with 30 mM
368 iodoacetamide (IA) for 30 min in the dark without shaking at room
369 temperature. Subsequently, 10 mM DTT was added to each sample, followed
370 by a quick vortex, and incubation for 10 min at room temperature without
371 shaking.

372 Total proteome peptide pools were generated using a KingFisher Duo
373 (ThermoScientific) automated sample preparation device as outlined by
374 Leutert et al. (2019)[36] without deviation. Sample digestion was performed
375 using sequencing grade trypsin (V5113; Promega), with generated peptide
376 pools quantified by Nanodrop, acidified with formic acid to a final
377 concentration of 5% (v/v) and then dried by vacuum centrifugation.
378 Peptides were then dissolved in 3% ACN/0.1% TFA, desalted using ZipTip
379 C18 pipette tips (ZTC18S960; Millipore) as previously described[7], then dried
380 and dissolved in 3.0% ACN/0.1% FA prior to MS analysis.

381 HeLa proteome analysis was carried out using a HeLa Protein Digest
382 Standard (88329; Pierce). Four replicate injections of this digest per analysis
383 type were carried out with the same methods as for Arabidopsis cell samples.

384 ## Nanoflow LC-MS/MS analysis

385 Peptide samples were analyzed using a Fusion Lumos Tribrid Orbitrap mass
386 spectrometer (ThermoScientific) in data dependent acquisition (DDA) and
387 data independent acquisition (DIA) modes. Dissolved peptides (1 µg) were
388 injected using an Easy-nLC 1200 system (LC140; ThermoScientific) and
389 separated on a 50 cm Easy-Spray PepMap C18 Column (ES803A;
390 ThermoScientific). The column was equilibrated with 100% solvent A (0.1%

formic acid (FA) in water). Common MS settings between DDA and DIA runs included a spray voltage of 2.2 kV, funnel RF level of 40 and heated capillary at 300°C. All data were acquired in profile mode using positive polarity with peptide match off and isotope exclusion selected. All gradients were run at 300 nL/min with analytical column temperature set to 50°C.

DDA acquisition: Peptides were eluted with a solvent B gradient (0.1% (v/v) FA in 80% (v/v) ACN): 4% - 41% B (0 – 120 min); 41% - 98% B (120-125 min). DDA acquisition was performed using the Universal Method (ThermoScientific). Full scan MS^1 spectra (350 - 2000 m/z) were acquired with a resolution of 120,000 at 200m/z with a normalized AGC Target of 125% and a maximum injection time of 50 ms. DDA MS^2 were acquired in the linear ion trap using quadrupole isolation in a window of 2.5 m/z. Selected ions were HCD fragmented with 35% fragmentation energy, with the ion trap run in rapid scan mode with an AGC target of 200% and a maximum injection time of 100 ms. Precursor ions with a charge state of +2 - +7 and a signal intensity of at least $5.0e^3$ were selected for fragmentation. All precursor signals selected for MS/MS were dynamically excluded for 30s.

DIA acquisition: Peptides were eluted using a segmented solvent B gradient of 0.1% (v/v) FA in 80% (v/v) ACN from 4% - 41% B (0 - 107 min). DIA acquisition was performed as per Bekker-Jensen et al. (2020)[20] and Biognosys AG. Full scan MS^1 spectra (350 - 1400 m/z) were acquired with a resolution of 120,000 at 200 m/z with a normalized AGC Target of 250% and a maximum injection time of 45 ms. ACG target value for fragment spectra was set to 2000%. Twenty-eight 38.5 m/z windows were used with an overlap of 1 m/z **(Supplementary Table 21)**. Resolution was set to 30,000 using a dynamic maximum injection time and a minimum number of desired points across each peak set to 6.

BoxCar DIA acquisition was performed using the same gradient settings as DIA acquisition outlined above. MS^1 analysis was performed by using two multiplexed targeted SIM scans of 10 BoxCar windows each. Detection was performed at 120,000 and normalized AGC targets of 100% per BoxCar isolation window. Isolation windows used are described in Supplementary Table 22. Windows were designed using the custom boxcarmaker R script that divides the MS1 spectra list into 20 m/z bins, each with an equal number of precursors, using the equal_freq function in the funModeling package (http://pablo14.github.io/funModeling/).

MS^2 acquisition was performed according to the settings described above for DIA acquisition.

Raw data processing

DDA files were processed using MaxQuant software version 1.6.14[29,30]. MS/MS spectra were searched with the Andromeda search engine against a custom made decoyed (reversed) version of the Arabidopsis protein

database from Araport 11[37] concatenated with a collection of 261 known mass spectrometry contaminants. Trypsin specificity was set to two missed cleavage and a protein and PSM false discovery rate of 1%; respectively. Minimal peptide length was set to seven and match between runs option enabled. Fixed modifications included carbamidomethylation of cysteine residues, while variable modifications included methionine oxidation.

DIA files were processed with the Spectronaut directDIA experimental analysis workflow using default settings without N-acetyl variable modification enabled. Trypsin specificity was set to two missed cleavages and a protein and PSM false discovery rate of 1%; respectively. Data filtering was set to Q-value and global normalization. For comparing BoxCarDIA and directDIA, the Spectronaut directDIA workflow was used with factory settings.

For hybrid (library- and library-free) DIA analysis, DDA raw files were first searched with the Pulsar search engine implemented in Spectronaut 14 to produce a search archive. Next, the DIA files were searched along with this search archive to generate a spectral library. The spectral library was then used for normal DIA analysis in Spectronaut 14. Default settings (without N-acetyl variable modification) were used in all steps. Final optimized Excalibur method files for DDA, directDIA and BoxCarDIA are provided as Supplemental Information.

Data analysis

Downstream data analysis for DDA samples was performed using Perseus version 1.6.14.0[38]. Reverse hits and contaminants were removed, the data log_2-transformed, followed by a data sub-selection criterion of n=3 of 4 replicates in at least one sample. Missing values were replaced using the normal distribution imputation method with default settings to generate a list of reliably quantified proteins. Subsequently, significantly changing differentially abundant proteins were determined and corrected for multiple comparisons (Bonferroni-corrected p-value < 0.05; q-value).

DirectDIA and BoxCarDIA data analysis was performed on Spectronaut v.14 using default settings.

Statistical analysis and plotting were performed using GraphPad Prism 8. Network analysis was performed on Cytoscape v.3.8.0 using the StringDB plugin.

Data availability

Raw data have been deposited to the ProteomeExchange Consortium (http://proteomecentral.proteomexchange.org) via the PRIDE partner repository with the dataset identifier PXD022448. Source data used to produce all graphs is provided in the Supplemental Materials. R scripts and input data used can be downloaded from:

https://github.com/UhrigLab/BoxCarMaker under a GNU Affero General Public License 3.0.

Acknowledgements

The authors thank Jack Moore (University of Alberta) for assistance with operating the mass-spectrometer. We are grateful to Fabia Simona and Oliver Bernhardt (Biognosys AG) for assistance troubleshooting the Spectronaut software analysis, and to Florian Meier (Max Planck Institute for Biochemistry) for advice on BoxCar acquisition.

Author Information

Affiliations

Department of Biological Sciences, University of Alberta, Edmonton T6G 2E9, Alberta, Canada

Devang Mehta, Sabine Scandola, R. Glen Uhrig

Contributions

D.M., and R.G.U contributed to Conceptualization, Methodology, and Formal Analysis. D.M. and S.S. contributed to Investigation. D.M. contributed to Visualization and Writing (original draft). R.G.U. performed Supervision and Funding Acquisition. D.M., S.S., and R.G.U contributed to Writing (review & editing).

Corresponding author

Dr. R. Glen Uhrig: ruhrig@ualberta.ca

Ethics Declarations

Conflict of Interest

The authors declare no conflict of interest

References

1. Mehta, D. et al. Phosphate and phosphite differentially impact the proteome and phosphoproteome of Arabidopsis suspension cell cultures. Plant J. Accepted, (2020).

2. Clark, N. M. et al. Integrated omics networks reveal the temporal signaling events of brassinosteroid response in Arabidopsis. BioRxiv (2020). doi:10.1101/2020.09.04.283788

3. Vanderschuren, H. et al. Large-Scale Proteomics of the Cassava Storage Root and Identification of a Target Gene to Reduce Postharvest Deterioration. Plant Cell 26, 1913–1924 (2014).

4. Ting, L., Rad, R., Gygi, S. P. & Haas, W. MS3 eliminates ratio distortion in isobaric multiplexed quantitative proteomics. Nat. Methods 8, 937–940 (2011).

5. Ow, S. Y. et al. iTRAQ underestimation in simple and complex mixtures: “the good, the bad and the ugly”. J. Proteome Res. 8, 5347–5355 (2009).

6. Graf, A. et al. Parallel analysis of Arabidopsis circadian clock mutants reveals different scales of transcriptome and proteome regulation. Open Biol 7, (2017).

7. Uhrig, R. G., Schläpfer, P., Roschitzki, B., Hirsch-Hoffmann, M. & Gruissem, W. Diurnal changes in concerted plant protein phosphorylation and acetylation in Arabidopsis organs and seedlings. Plant J. 99, 176–194 (2019).

8. Hartl, M. et al. Lysine acetylome profiling uncovers novel histone deacetylase substrate proteins in Arabidopsis. Mol. Syst. Biol. 13, 949 (2017).

9. Aebersold, R. & Mann, M. Mass-spectrometric exploration of proteome structure and function. Nature 537, 347–355 (2016).

10. Gillet, L. C. et al. Targeted data extraction of the MS/MS spectra generated by data-independent acquisition: a new concept for consistent and accurate proteome analysis. Mol. Cell Proteomics 11, O111.016717 (2012).

11. Ludwig, C. et al. Data-independent acquisition-based SWATH-MS for quantitative proteomics: a tutorial. Mol. Syst. Biol. 14, e8126 (2018).

12. Tsou, C.-C. et al. DIA-Umpire: comprehensive computational framework for data-independent acquisition proteomics. Nat. Methods 12, 258–64, 7 p following 264 (2015).

13. Li, Y. et al. Group-DIA: analyzing multiple data-independent acquisition mass spectrometry data files. Nat. Methods 12, 1105–1106 (2015).

14. Biognosys AG. A new era in proteomics: spectral library free data independent acquisition (directDIA). The Analytical Scientist (2017).

15. Bruderer, R., Bernhardt, O. M., Gandhi, T. & Reiter, L. High-precision iRT prediction in the targeted analysis of data-independent acquisition and its impact on identification and quantitation. Proteomics 16, 2246–2256 (2016).

16. Reiter, L. MP 125: Direct Searching of DIA Data Catches up with Sample-specific Libraries. in Proceedings of the 68th ASMS Conference on Mass Spectrometry and Allied Topics, Online Meeting (American Society for Mass Spectrometry, 2020). at <https://biognosys.com/media.ashx/mp125lukasreiterasms2020.pdf>

17. Yang, Y. et al. In silico spectral libraries by deep learning facilitate data-independent acquisition proteomics. Nat. Commun. 11, 146 (2020).

18. Demichev, V., Messner, C. B., Vernardis, S. I., Lilley, K. S. & Ralser, M. DIA-NN: neural networks and interference correction enable deep proteome coverage in high throughput. Nat. Methods 17, 41–44 (2020).

19. Muntel, J. et al. Surpassing 10 000 identified and quantified proteins in a single run by optimizing current LC-MS instrumentation and data analysis strategy. Mol. Omics 15, 348–360 (2019).

20. Bekker-Jensen, D. B. et al. Rapid and site-specific deep phosphoproteome profiling by data-independent acquisition without the need for spectral libraries. Nat. Commun. 11, 787 (2020).

21. Meier, F., Geyer, P. E., Virreira Winter, S., Cox, J. & Mann, M. BoxCar acquisition method enables single-shot proteomics at a depth of 10,000 proteins in 100 minutes. Nat. Methods 15, 440–448 (2018).

22. Van Leene, J. et al. Capturing the phosphorylation and protein interaction landscape of the plant TOR kinase. Nat. Plants 5, 316–327 (2019).

23. Van Leene, J. et al. Targeted interactomics reveals a complex core cell cycle machinery in Arabidopsis thaliana. Mol. Syst. Biol. 6, 397 (2010).

24. Gonzalez, N. et al. A repressor protein complex regulates leaf growth in arabidopsis. Plant Cell 27, 2273–2287 (2015).

25. Antosz, W. et al. The Composition of the Arabidopsis RNA Polymerase II Transcript Elongation Complex Reveals the Interplay between Elongation and mRNA Processing Factors. Plant Cell 29, 854–870 (2017).

26. Dejonghe, W. et al. Disruption of endocytosis through chemical inhibition of clathrin heavy chain function. Nat. Chem. Biol. 15, 641–649 (2019).

27. Marondedze, C., Thomas, L., Serrano, N. L., Lilley, K. S. & Gehring, C. The RNA-binding protein repertoire of Arabidopsis thaliana. Sci. Rep. 6, 29766 (2016).

28. Arora, D. et al. Establishment of Proximity-dependent Biotinylation Approaches in Different Plant Model Systems. Plant Cell (2020). doi:10.1105/tpc.20.00235

29. Cox, J. & Mann, M. MaxQuant enables high peptide identification rates, individualized p.p.b.-range mass accuracies and proteome-wide protein quantification. Nat. Biotechnol. 26, 1367–1372 (2008).

30. Tyanova, S., Temu, T. & Cox, J. The MaxQuant computational platform for mass spectrometry-based shotgun proteomics. Nat. Protoc. 11, 2301–2319 (2016).

31. Lex, A., Gehlenborg, N., Strobelt, H., Vuillemot, R. & Pfister, H. Upset: visualization of intersecting sets. IEEE Trans Vis Comput Graph 20, 1983–1992 (2014).

32. Szklarczyk, D. et al. STRING v11: protein-protein association networks with increased coverage, supporting functional discovery in genome-wide experimental datasets. Nucleic Acids Res. 47, D607–D613 (2019).

33. Grinfeld, D., Aizikov, K., Kreutzmann, A., Damoc, E. & Makarov, A. Phase-Constrained Spectrum Deconvolution for Fourier Transform Mass Spectrometry. Anal. Chem. 89, 1202–1211 (2017).

34. Meier, F. High Dynamic Range Proteome Analysis with BoxCar DIA and Super-Resolution Orbitrap Mass Spectrometry. (2020). at <http://assets.thermofisher.com/TFS-Assets/CMD/posters/po-65792-ms-proteome-boxcar-dia-orbitrap-asms2020-po65792-en.pdf>

35. Uhrig, R. G. & Moorhead, G. B. Two ancient bacterial-like PPP family phosphatases from Arabidopsis are highly conserved plant proteins that possess unique properties. Plant Physiol. 157, 1778–1792 (2011).

36. Leutert, M., Rodríguez-Mias, R. A., Fukuda, N. K. & Villén, J. R2-P2 rapid-robotic phosphoproteomics enables multidimensional cell signaling studies. Mol. Syst. Biol. 15, e9021 (2019).

37. Cheng, C.-Y. et al. Araport11: a complete reannotation of the Arabidopsis thaliana reference genome. Plant J. 89, 789–804 (2017).

38. Tyanova, S. et al. The Perseus computational platform for comprehensive analysis of (prote)omics data. Nat. Methods 13, 731–740 (2016).

Supplementary Tables

Supplementary Table 1: DDA protein quantification results for Arabidopsis cells

Supplementary Table 2: directDIA protein quantification results for Arabidopsis cells

Supplementary Table 3: Comparison of protein quantification for Arabidopsis cells between DDA and directDIA

Supplementary Table 4: DDA protein quantification results for HeLa digests

Supplementary Table 5: directDIA protein quantification results for HeLa digests

Supplementary Table 6: BoxCarDIA protein quantification results for Arabidopsis cells

Supplementary Table 7: directDIA protein quantification results for Arabidopsis cells in a second experiment for comparison with directDIA

Supplementary Table 8: Proteins identified in Arabidopsis cells using DDA

Supplementary Table 9: directDIA protein quantification results for Arabidopsis cells filtered for valid values in 3 of 4 replicates.

Supplementary Table 10: DDA protein quantification results for Arabidopsis cells with no imputation

Supplementary Table 11: directDIA protein quantification results for Arabidopsis cells filtered for valid values in all replicates.

Supplementary Table 12: DDA protein quantification results for Arabidopsis cells filtered for valid values in all replicates.

Supplementary Table 13: Proteins identified in HeLa digests using DDA

Supplementary Table 14: directDIA protein quantification results for HeLa digests filtered for valid values in 3 of 4 replicates.

Supplementary Table 15: DDA protein quantification results for HeLa digests with no imputation

Supplementary Table 16: directDIA protein quantification results for HeLa digests filtered for valid values in all replicates.

Supplementary Table 17: DDA protein quantification results for HeLa digests filtered for valid values in all replicates.

Supplementary Table 18: BoxCarDIA protein quantification results for HeLa digests

Supplementary Table 19: directDIA protein quantification results for HeLa digests in a second experiment for comparison with BoxCarDIA

Supplementary Table 20: Proteins changing significantly in abundance between light and dark-grown Arabidopsis cells, measured using both directDIA and DDA.

Supplementary Table 21: Precursor selection mass list table

Supplementary Table 22: BoxCar isolation windows

Supplementary Figures

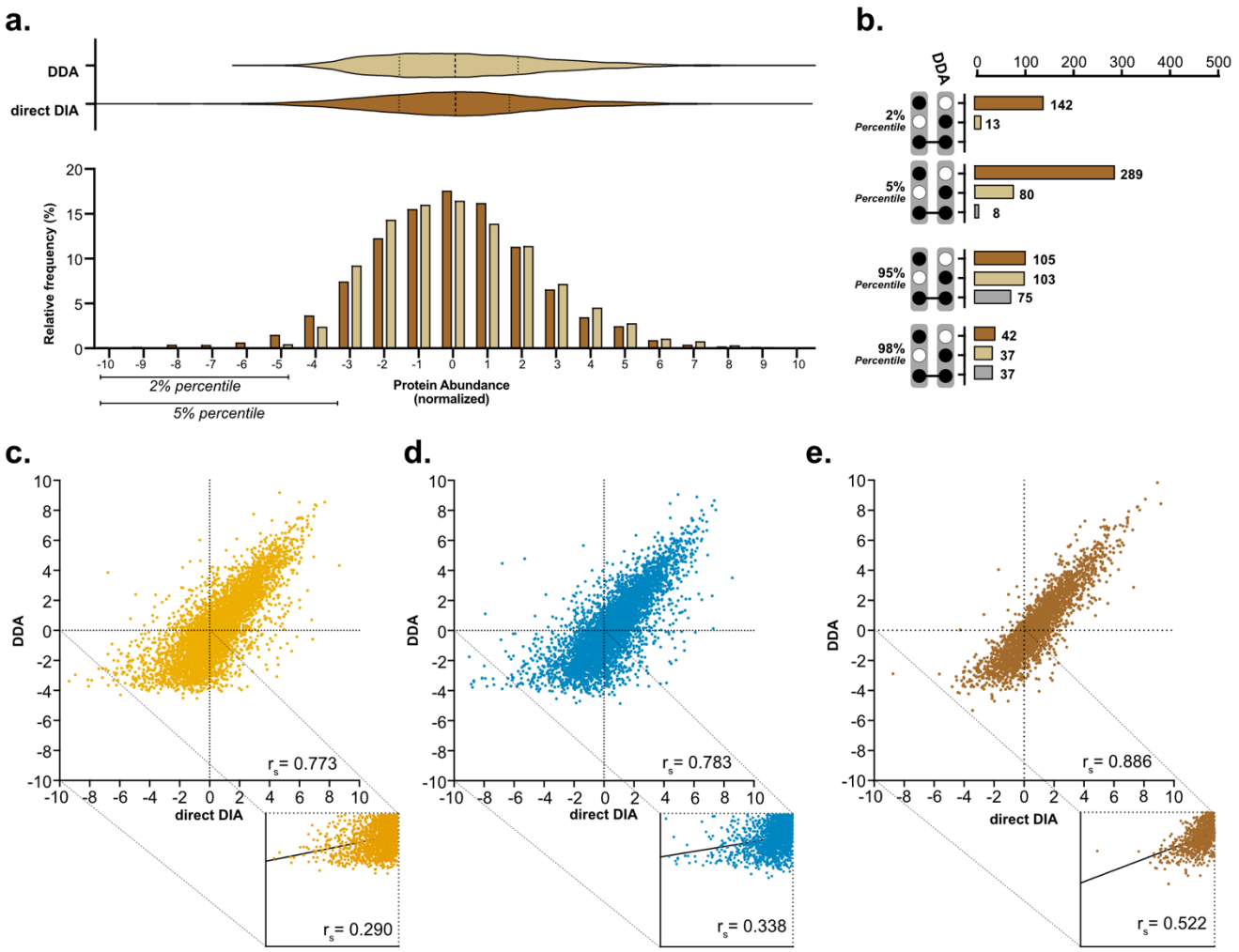

Figure S1: Comparison of protein quantification results using DDA and directDIA analysis.
(a.) Frequency distribution of normalized protein abundances for DDA and directDIA analysis and corresponding violin plots with median and quartile lines marked for HeLa digests. **(b.)** Upset plots depicting intersections in protein groups quantified by DDA and direct DIA at either extreme of the abundance distribution for HeLa digests. **(c.-e.)** Scatter plots of protein groups quantified by DDA and direct DIA for light-grown Arabidopsis cells, dark-grown Arabidopsis cells, and HeLa digests. Insets show correlations for protein groups with abundances less than the median.

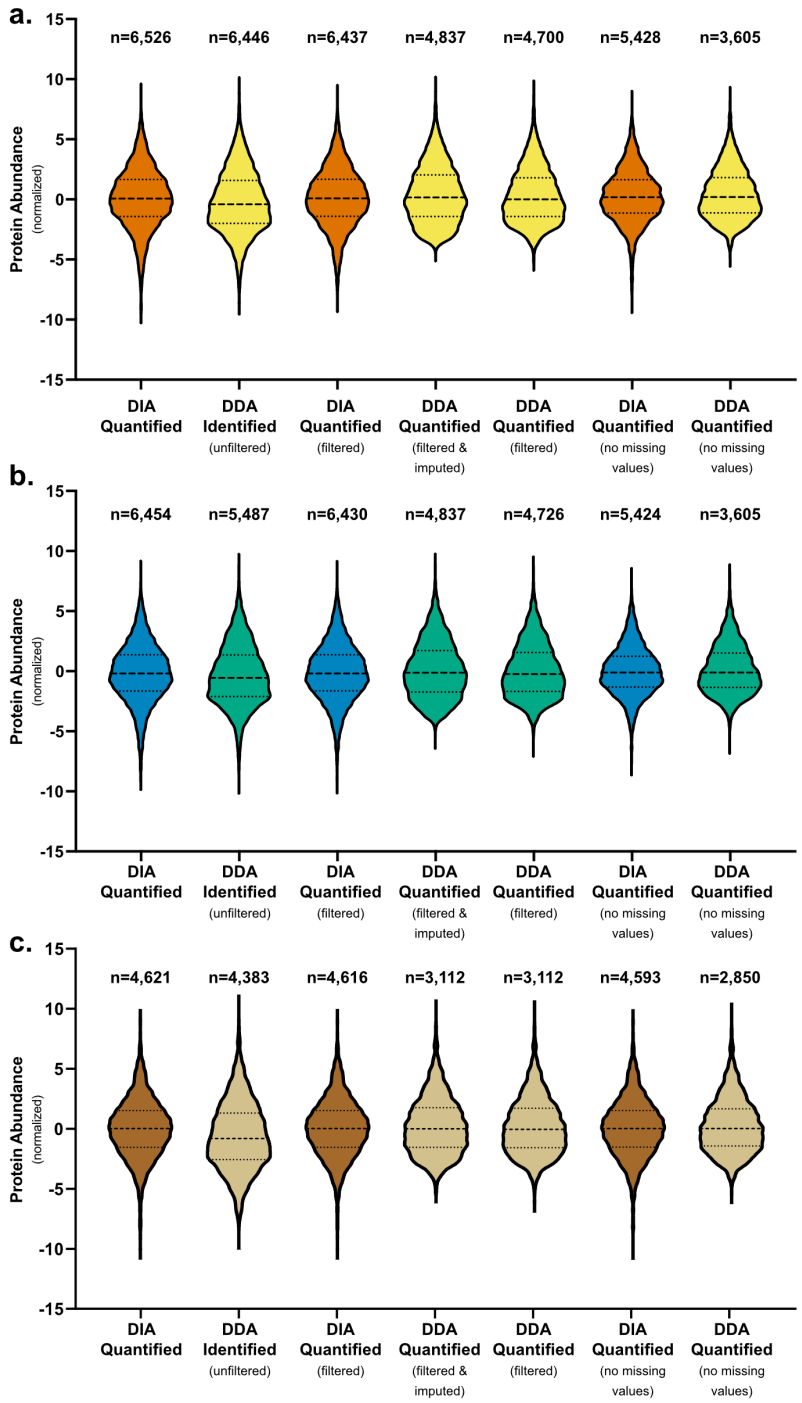

Figure S2: Protein abundance distributions by analysis type and data filtering settings.

Violin plots showing normalized protein abundance for proteins quantified by direct DIA (default setting), identified by DDA, quantified by DIA (filtered for protein groups present in at least 3 samples in any one condition), quantified by DDA (filtered for protein groups present in at least 3 samples in any one condition with missing values imputed), quantified by DDA (filtered for protein groups present in at least 3 samples in any one condition with missing values left blank), quantified by DIA (counting only protein groups found in all samples), and quantified by DIA (counting only protein groups found in all samples), respectively for **(a.)** light grown Arabidopsis cells **(b.)** dark grown Arabidopsis cells and **(c.)** HeLa cell digestion standards. (n= number of protein groups).

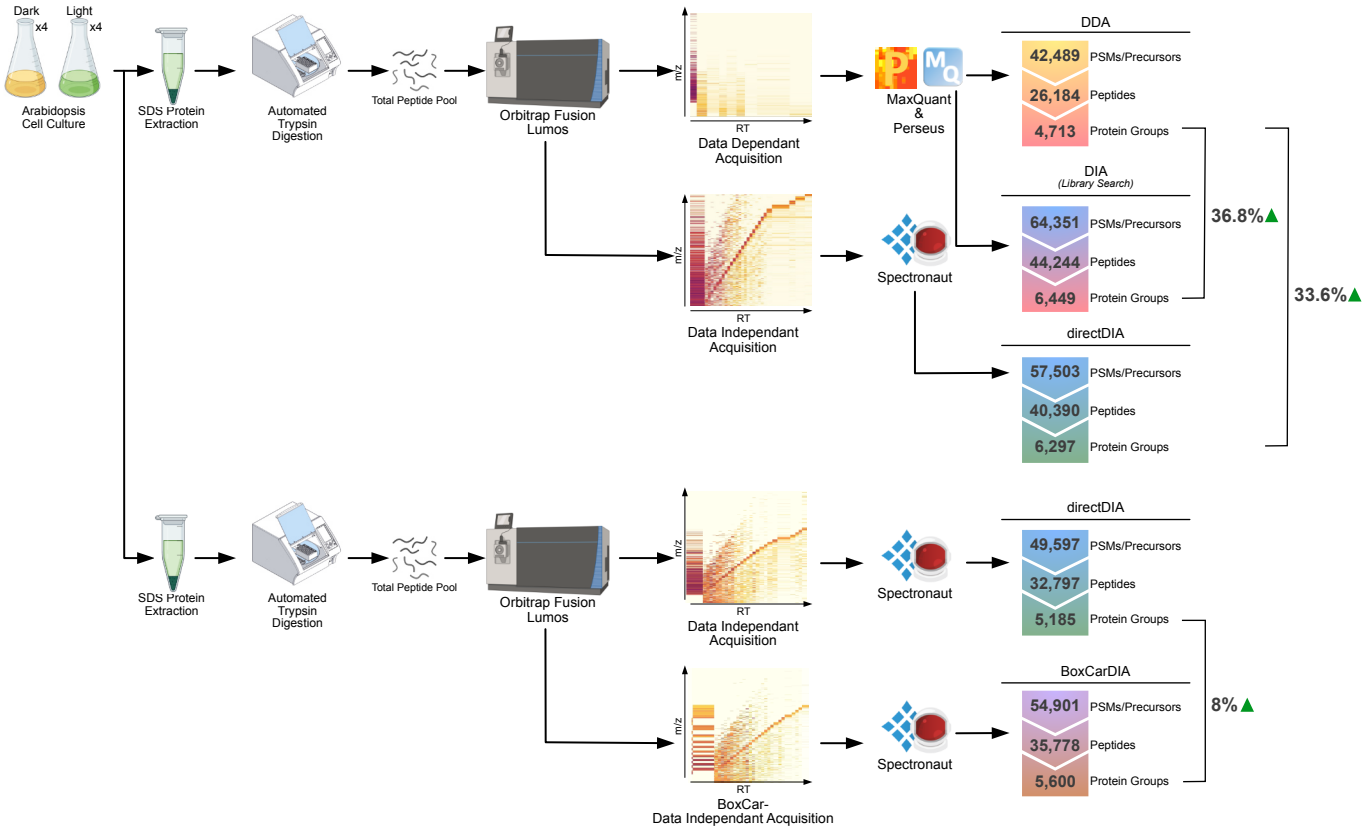
Dark
x4
Light
x4
Arabidopsis
Cell Culture
SDS Protein
Extraction
Automated
Trypsin
Digestion
Total Peptide Pool
Orbitrap Fusion
Lumos
m/z
RT
Data Dependant
Acquisition
Data Independant
Acquisition
MaxQuant
&
Perseus
Spectronaut
DDA
42,489 PSMs/Precursors
26,184 Peptides
4,713 Protein Groups
DIA
(Library Search)
64,351 PSMs/Precursors
44,244 Peptides
6,449 Protein Groups
directDIA
57,503 PSMs/Precursors
40,390 Peptides
6,297 Protein Groups
36.8%▲
33.6%▲
SDS Protein
Extraction
Automated
Trypsin
Digestion
Total Peptide Pool
Orbitrap Fusion
Lumos
Data Independant
Acquisition
BoxCar-
Data Independant Acquisition
Spectronaut
Spectronaut
directDIA
49,597 PSMs/Precursors
32,797 Peptides
5,185 Protein Groups
BoxCarDIA
54,901 PSMs/Precursors
35,778 Peptides
5,600 Protein Groups
8%▲

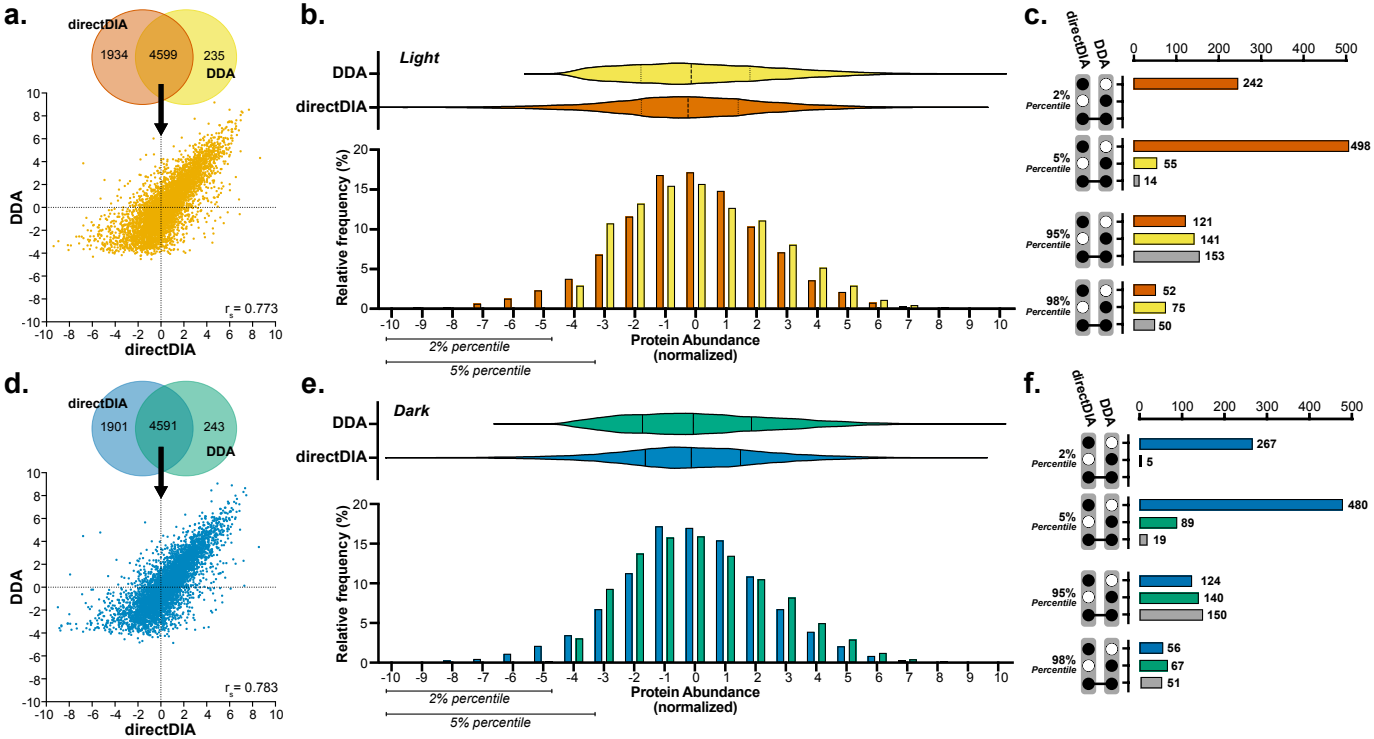
a.
directDIA
1934
4599
235
DDA
DDA
directDIA
r_s = 0.773
b.
Light
DDA
directDIA
Relative frequency (%)
Protein Abundance
(normalized)
2% percentile
5% percentile
c.
directDIA
DDA
2%
Percentile
242
5%
Percentile
498
55
14
95%
Percentile
121
141
153
98%
Percentile
52
75
50
d.
directDIA
1901
4591
243
DDA
DDA
directDIA
r_s = 0.783
e.
Dark
DDA
directDIA
Relative frequency (%)
Protein Abundance
(normalized)
2% percentile
5% percentile
f.
directDIA
DDA
2%
Percentile
267
5
5%
Percentile
480
89
19
95%
Percentile
124
140
150
98%
Percentile
56
67
51

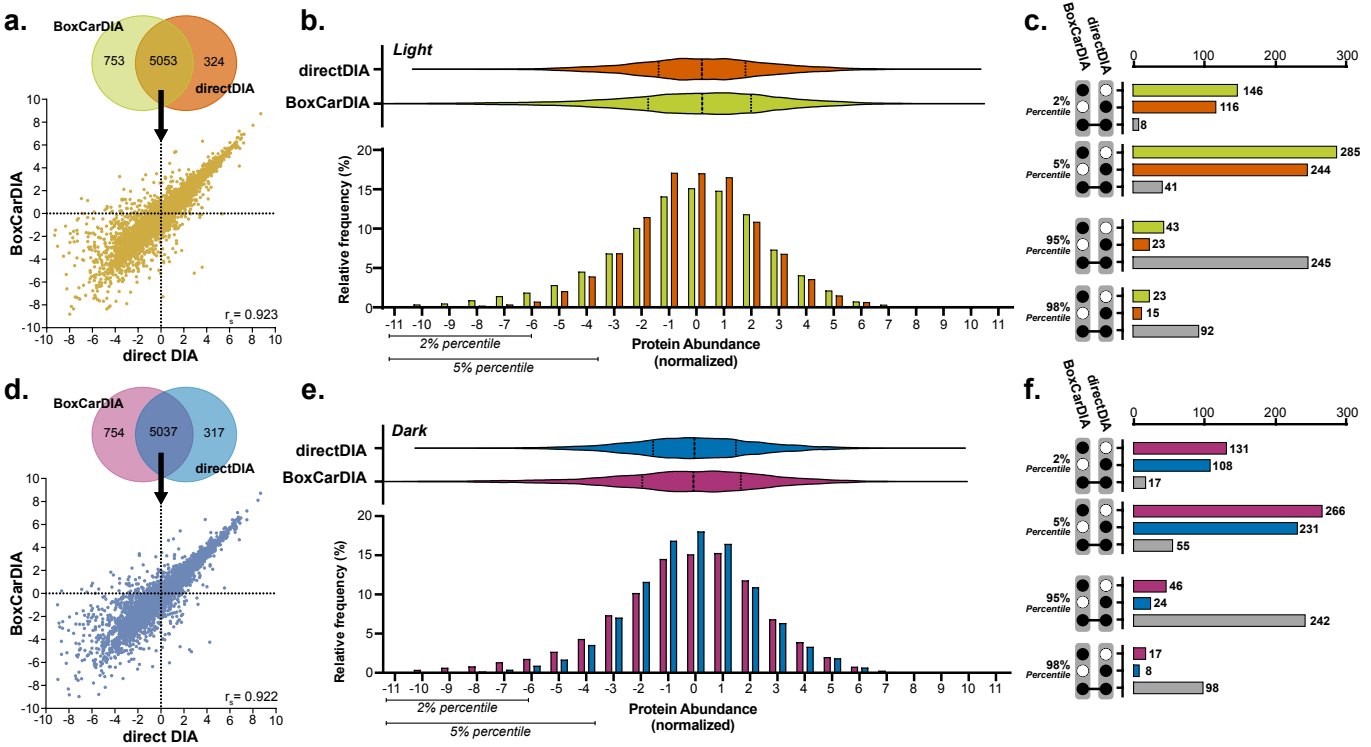
a.
BoxCarDIA
753
5053
324
directDIA
BoxCarDIA
direct DIA
r_s = 0.923
b.
Light
directDIA
BoxCarDIA
Relative frequency (%)
2% percentile
5% percentile
Protein Abundance
(normalized)
c.
BoxCarDIA
directDIA
2% Percentile
146
116
8
5% Percentile
285
244
41
95% Percentile
43
23
245
98% Percentile
23
15
92
d.
BoxCarDIA
754
5037
317
directDIA
BoxCarDIA
direct DIA
r_s = 0.922
e.
Dark
directDIA
BoxCarDIA
Relative frequency (%)
2% percentile
5% percentile
Protein Abundance
(normalized)
f.
BoxCarDIA
directDIA
2% Percentile
131
108
17
5% Percentile
266
231
55
95% Percentile
46
24
242
98% Percentile
17
8
98

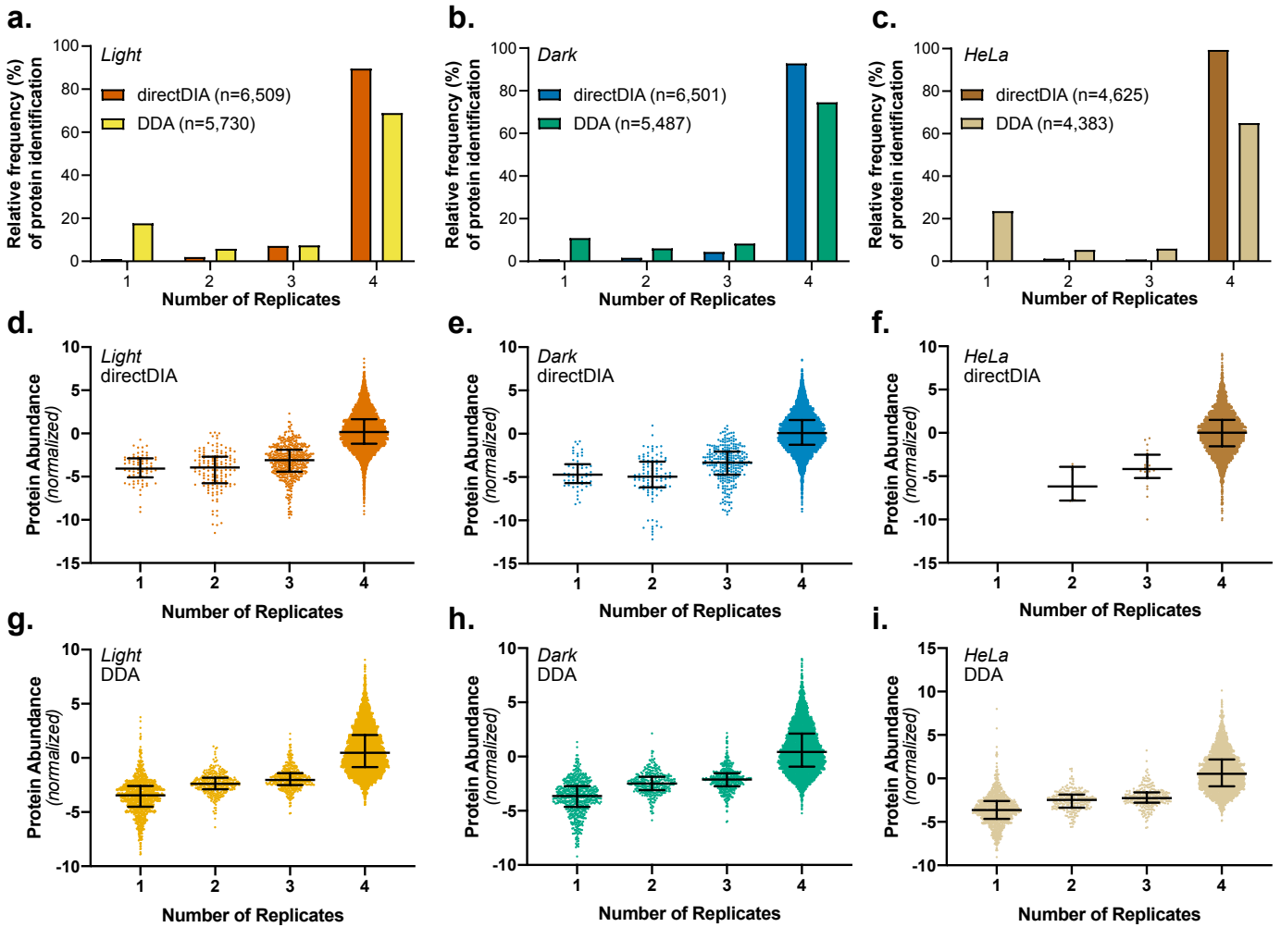
a.
Light
directDIA (n=6,509)
DDA (n=5,730)
Relative frequency (%) of protein identification
Number of Replicates
b.
Dark
directDIA (n=6,501)
DDA (n=5,487)
Relative frequency (%) of protein identification
Number of Replicates
c.
HeLa
directDIA (n=4,625)
DDA (n=4,383)
Relative frequency (%) of protein identification
Number of Replicates
d.
Light
directDIA
Protein Abundance (normalized)
Number of Replicates
e.
Dark
directDIA
Protein Abundance (normalized)
Number of Replicates
f.
HeLa
directDIA
Protein Abundance (normalized)
Number of Replicates
g.
Light
DDA
Protein Abundance (normalized)
Number of Replicates
h.
Dark
DDA
Protein Abundance (normalized)
Number of Replicates
i.
HeLa
DDA
Protein Abundance (normalized)
Number of Replicates

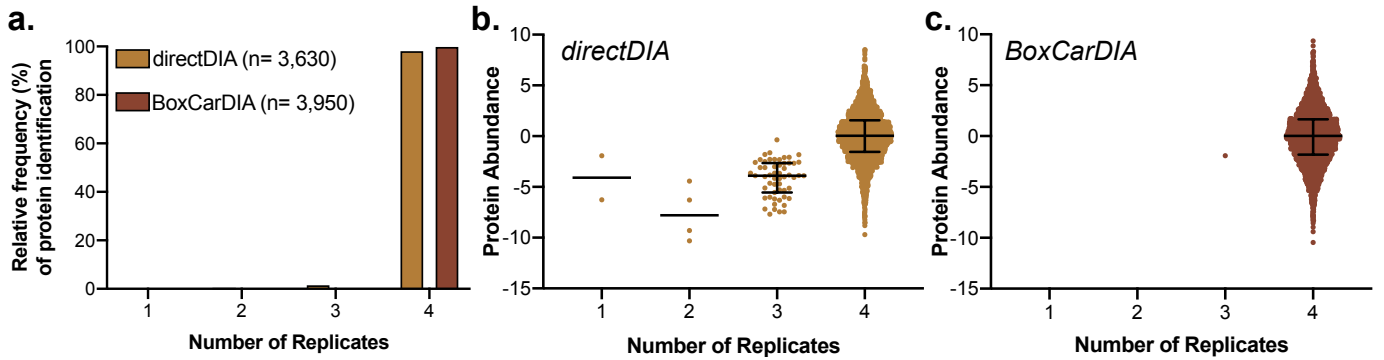
a.
directDIA (n= 3,630)
BoxCarDIA (n= 3,950)
Relative frequency (%) of protein identification
100
80
60
40
20
0
1
2
3
4
Number of Replicates
b.
directDIA
Protein Abundance
10
5
0
-5
-10
-15
1
2
3
4
Number of Replicates
c.
BoxCarDIA
Protein Abundance
10
5
0
-5
-10
-15
1
2
3
4
Number of Replicates

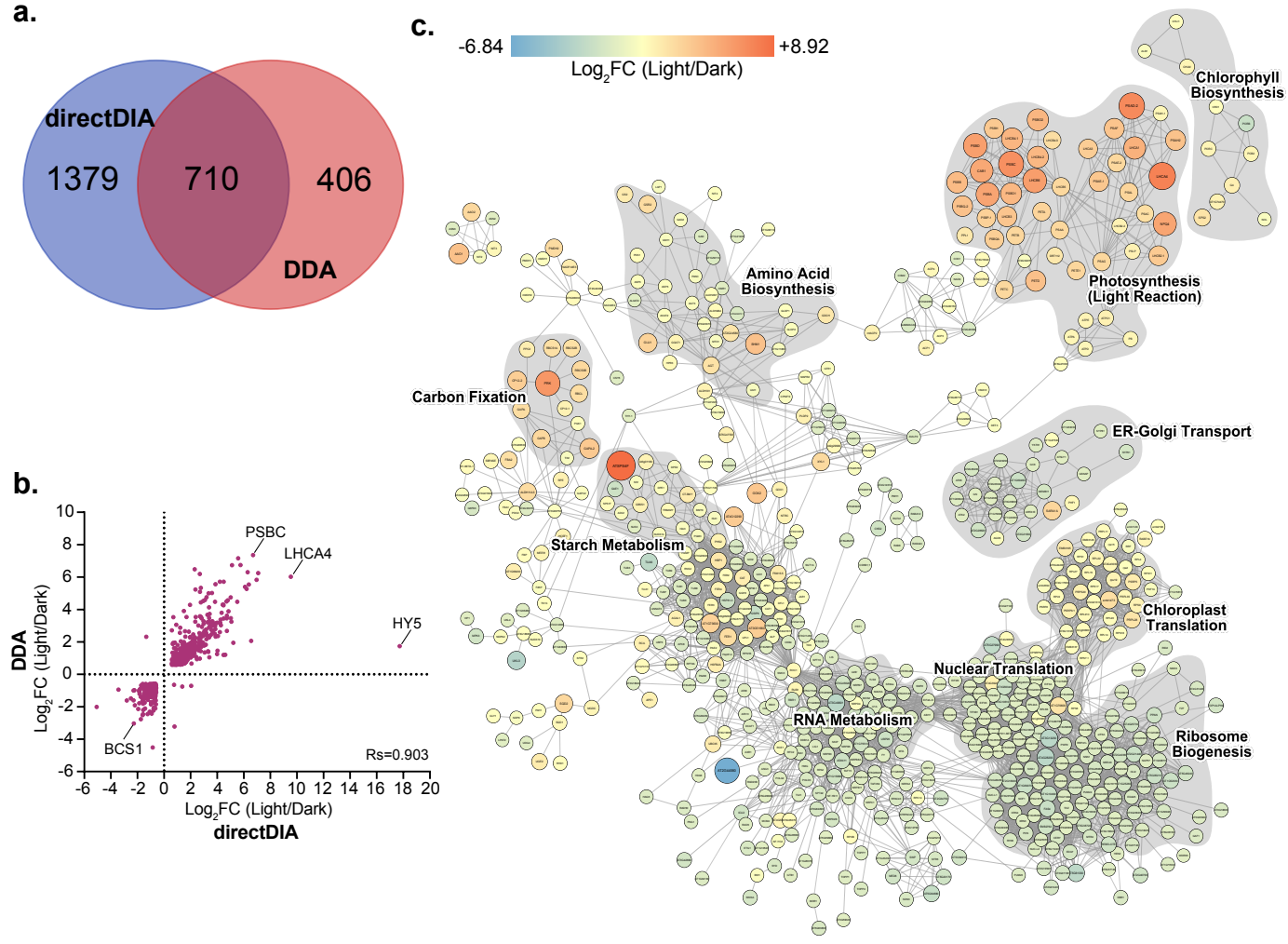
a.
directDIA
1379
710
406
DDA
b.
PSBC
LHCA4
HY5
BCS1
Rs=0.903
DDA
Log2FC (Light/Dark)
directDIA
Log2FC (Light/Dark)
c.
-6.84
+8.92
Log2FC (Light/Dark)
Chlorophyll Biosynthesis
Amino Acid Biosynthesis
Photosynthesis (Light Reaction)
Carbon Fixation
ER-Golgi Transport
Starch Metabolism
Chloroplast Translation
Nuclear Translation
RNA Metabolism
Ribosome Biogenesis